



Check for updates

Condensed Matter Physics.
Semiconductor Physics

UDC 538.9

<https://www.doi.org/10.33910/2687-153X-2021-2-2-61-67>

Local structure of amorphous and crystalline $\text{Ge}_2\text{Sb}_2\text{Te}_5$ films

Yu. A. Petrushin¹, A. V. Marchenko¹, P. P. Seregin^{✉1}

¹ Herzen State Pedagogical University of Russia, 48 Moika Emb., Saint Petersburg 191186, Russia

Authors

Yuri A. Petrushin, e-mail: uraordie@mail.ru

Alla V. Marchenko, ORCID: [0000-0002-9292-2541](https://orcid.org/0000-0002-9292-2541), e-mail: al7140@rambler.ru

Pavel P. Seregin, ORCID: [0000-0001-5004-2047](https://orcid.org/0000-0001-5004-2047), e-mail: ppseregin@mail.ru

For citation: Petrushin, Yu. A., Marchenko, A. V., Seregin, P. P. (2021) Local structure of amorphous and crystalline $\text{Ge}_2\text{Sb}_2\text{Te}_5$ films. *Physics of Complex Systems*, 2 (2), 61–67. <https://www.doi.org/10.33910/2687-153X-2021-2-2-61-67>

Received 10 February 2021; reviewed 10 March 2021; accepted 10 March 2021.

Copyright: © The Authors (2021). Published by Herzen State Pedagogical University of Russia. Open access under [CC BY-NC License 4.0](https://creativecommons.org/licenses/by-nc/4.0/)

Abstract. An effective way to examine structural rearrangement in solids is Mössbauer spectroscopy. A key requirement to Mössbauer probes used for these purposes is the possibility of their localization in a certain site of the crystal lattice or in the structural network of the amorphous material. When absorption spectroscopy is used to examine the local structure of crystalline and amorphous $\text{Ge}_2\text{Sb}_2\text{Te}_5$ films, this requirement is satisfied for ^{119}Sn isotope. Tin atoms ^{119}Sn isovalently substitute germanium atoms in the structure of both vitreous and crystalline germanium tellurides. The absorption Mössbauer spectroscopy on ^{119}Sn impurity centers shows that germanium atoms in the structure of amorphous and polycrystalline $\text{Ge}_2\text{Sb}_2\text{Te}_5$ films have different local symmetries (tetrahedral in the amorphous phase and octahedral in the crystalline).

Keywords: Mössbauer spectroscopy, phase-memory, $\text{Ge}_2\text{Sb}_2\text{Te}_5$, local structure, X-ray fluorescence analysis.

Introduction

Phase-memory (PM) devices based on chalcogenide semiconductors are mostly used at present for reversible transitions from the amorphous to the crystalline state of thin Ge—Sb—Te films, with the composition $\text{Ge}_2\text{Sb}_2\text{Te}_5$ attracting most interest. The compound $\text{Ge}_2\text{Sb}_2\text{Te}_5$ cannot be obtained as bulk glass, but the magnetron sputtering of a target can produce amorphous films. The improvement of PM devices and the technology of their production should be based on the results of a study of the crystallization of amorphous $\text{Ge}_2\text{Sb}_2\text{Te}_5$ films. Obtaining information about the local structure of an amorphous film and comparing it with the crystal structure is paramount to such studies. It is impossible to describe the PM mechanism without knowing the structural transformations in reversible phase transitions between the amorphous and crystalline states. For example, a model of a fast reversible transition from the crystalline to the amorphous state was suggested in the early studies of $\text{Ge}_2\text{Sb}_2\text{Te}_5$ films by the XANES method (X-ray absorption near-edge structure) (Kolobov et al. 2004).

The reversible transition from the amorphous state to the cubic crystalline phase is most frequently used in $\text{Ge}_2\text{Sb}_2\text{Te}_5$ -based PM devices. However, the operating temperatures of these devices are limited to 120 °C because of the low thermal stability of the amorphous phase. It was suggested in a recent study (Hu et al. 2020) to replace the amorphous-cubic phase transition with a transition from the metastable cubic to stable hexagonal phase in the same films. This replacement provides a combination of high optical contrast, thermal stability, and a small change in density. It also raises the maximum working temperature of optics to 240 °C. The authors of (Hu et al. 2020) attribute the high optical contrast to an increase in the difference in structural disorder on passing from the cubic phase to the hexagonal. This necessitates the analysis of the structure and structural disorder of both crystalline phases of $\text{Ge}_2\text{Sb}_2\text{Te}_5$.

An effective way to examine structural rearrangement in solids is Mossbauer spectroscopy (Bobokhuzhaev et al. 2020). A key requirement to Mössbauer probes used for these purposes is the possibility of their localization in a certain site of the crystal lattice or in the structural network of the amorphous material. When absorption spectroscopy is used to examine the local structure of crystalline and amorphous $\text{Ge}_2\text{Sb}_2\text{Te}_5$ films, this requirement is satisfied for ^{125}Te , ^{121}Sb as well as ^{119}Sn isotopes. ^{125}Te and ^{121}Sb can serve as probes for tellurium and antimony sites, whereas tin atoms ^{119}Sn isovalently substitute germanium atoms in the structure of both vitreous and crystalline germanium tellurides, as was previously shown (Seregina et al. 1977; Micoulaut et al. 2014; Marchenko et al. 2019). Additionally, it is possible to use emission Mössbauer spectroscopy for the ^{119m}Sn isotope with ^{119}Sb and ^{119m}Te parent nuclei. The parent nuclei are introduced into antimony and tellurium sites, respectively. The daughter Mössbauer probe ^{119m}Sn formed according to the decay scheme of ^{119}Sn and ^{119}Te in Fig. 1 can inherit either antimony sites (if the ^{119}Sb isotope is used) or tellurium sites (if the ^{119m}Te isotope is used). This process allows to obtain the models of antisite defects with tin (as an analog of germanium) at antimony or tellurium sites.

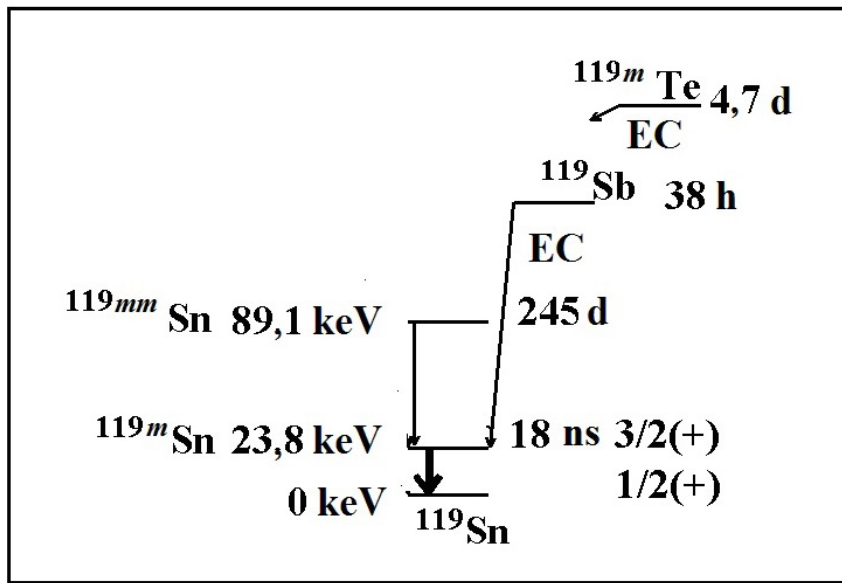


Fig. 1. Scheme of the decay of ^{119m}Sn , ^{119}Sb , and ^{119m}Te parent isotopes

In this study, we examine the structural rearrangements in $\text{Ge}_2\text{Sb}_2\text{Te}_5$ films by the above-described absorption and emission procedures. The goal of the study is to obtain information about the following:

- structural rearrangements in the local environment of germanium, antimony, and tellurium atoms during the crystallization of amorphous films;
- the nature of tin defects in the structure of crystalline films.

To interpret the obtained results, we also carry out similar studies of the crystalline compounds Sb_2Te_3 , GeTe , and vitreous alloy $\text{Ge}_{1.5}\text{Te}_{8.5}$.

Experiment

The compounds under study, $\text{Ge}_2\text{Sb}_2\text{Te}_5$, $\text{Ge}_{1.95}\text{Sn}_{0.05}\text{Sb}_2\text{Te}_5$, Sb_2Te_3 , and GeTe as well as $\text{Ge}_{1.45}\text{Sn}_{0.05}\text{Te}_{8.5}$ and $\text{Ge}_{1.5}\text{Te}_{8.5}$ alloys were synthesized from elementary substances at 1050 °C in quartz cells evacuated to 10^{-3} mm Hg.

X-ray-amorphous films of $\text{Ge}_2\text{Sb}_2\text{Te}_5$, $\text{Ge}_{1.95}\text{Sn}_{0.05}\text{Sb}_2\text{Te}_5$, $\text{Ge}_{1.45}\text{Sn}_{0.05}\text{Te}_{8.5}$, and $\text{Ge}_{1.5}\text{Te}_{8.5}$ were produced by dc magnetron sputtering of the target of the corresponding compositions in an atmosphere of nitrogen. The $\text{Ge}_{1.95}\text{Sn}_{0.05}\text{Sb}_2\text{Te}_5$ and $\text{Ge}_{1.45}\text{Sn}_{0.05}\text{Te}_{8.5}$ were deposited by using a ^{119}Sn preparation enriched to 92%. Amorphous $\text{Ge}_2\text{Sb}_2\text{Te}_5$ and $\text{Ge}_{1.95}\text{Sn}_{0.05}\text{Sb}_2\text{Te}_5$ films were crystallized at 150 °C (to give a cubic *fcc* (face-centered cubic) phase) or at 310 °C (to give a hexagonal *hcp* (hexagonal cubic) phase) (Kato, Tanaka 2005; Shelby, Raoux 2009; Siegrist et al. 2011; Sousa 2011). The amorphous $\text{Ge}_{1.5}\text{Te}_{8.5}$ and $\text{Ge}_{1.45}\text{Sn}_{0.05}\text{Te}_{8.5}$ films were crystallized at 250 °C.

Mössbauer ^{119m}Sn sources based on $\text{Ge}_2\text{Sb}_2\text{Te}_5$ crystalline films (*hcp* phase) were prepared via the diffusion of carrierless ^{119}Sb or ^{119m}Te isotopes into thin amorphous films at a temperature of 310 °C for 10 h. ^{119m}Sn Mössbauer sources based on Sb_2Te_3 and GeTe were prepared via fusion of the corresponding compound with carrierless ^{119}Sb or ^{119}Te in sealed cells.

The ^{119}Sb and ^{119}Te isotopes were produced, respectively, by the reactions $^{119}\text{Sn}(p, n)^{119}\text{Sb}$ and $^{117}\text{Sn}(\alpha, 2n)^{119m}\text{Te}$, with the subsequent chromatographic isolation of carrierless preparations ^{119}Sb and ^{119}Te .

The emission spectra were measured with CaSnO_3 as an absorber (surface density in terms of tin 5 mg/cm²). The spectrum of this absorber with a source of the same composition was a single line with a full width at the half-height $G = 0.79(1)$ mm/s, which was taken to be the instrumental width of the spectral line. For the sources prepared with ^{119m}Te , the spectra were measured after dynamic radioactive equilibrium between the ^{119}Sb and ^{119m}Te isotopes was attained. The isomer shift of the Mössbauer spectra of ^{119m}Sn and ^{119}Sn is presented relative to the CaSnO_3 absorber. All the Mössbauer spectra were measured with a CM 4201 TerLab spectrometer at 80 K.

The compositions of the amorphous and crystalline films as well as of the target were monitored by the X-ray fluorescence analysis.

Experimental results and their discussion

Data of the absorption Mössbauer spectroscopy on ^{119}Sn

The typical spectra of ^{119}Sn impurity atoms in amorphous (vitreous) and polycrystalline materials, shown in Figs. 2 and 3, are single broadened lines ($G \sim 1.15\text{--}1.35$ mm/s).

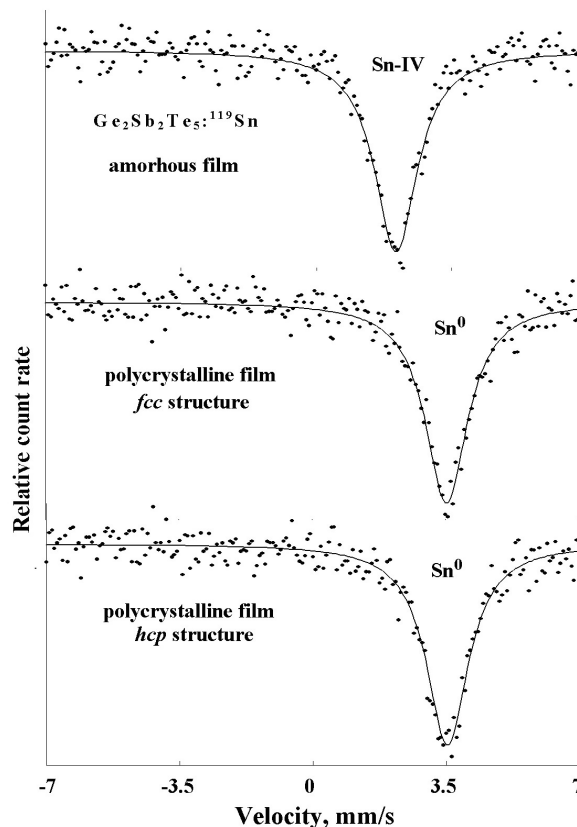


Fig. 2. Absorption Mössbauer spectra of Sn impurity atoms in amorphous and polycrystalline $\text{Ge}_2\text{Sb}_2\text{Te}_5$ films. The positions of spectral lines associated with Sn-IV and Sn⁰ centers

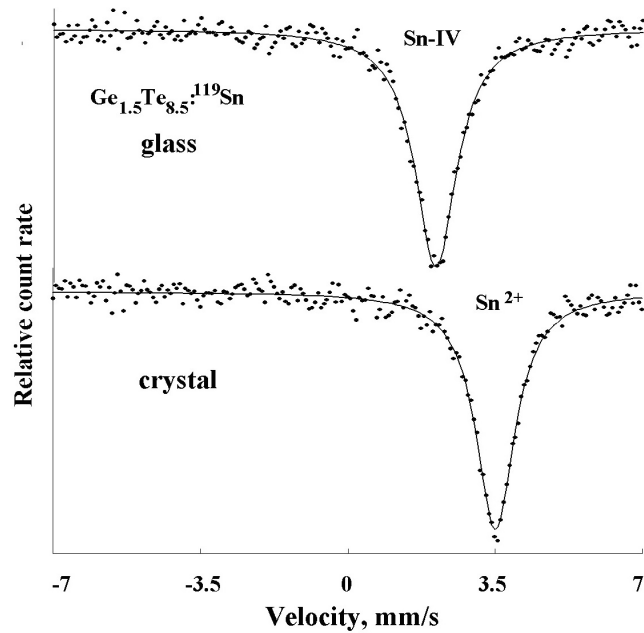


Fig. 3. Absorption Mössbauer spectra of ^{119}Sn impurity atoms in the vitreous and polycrystalline $\text{Ge}_{1.5}\text{Te}_{8.5}$ alloy. The positions of spectral lines associated with Sn-IV and Sn centers

The spectra of ^{119}Sn for amorphous $\text{Ge}_2\text{Sb}_2\text{Te}_5$ and vitreous $\text{Ge}_{x_5}\text{Te}_{8_5}$ show isomer shifts $IS \sim 2.06\text{--}2.09$ mm/s. These isomer shifts are typical of the spectra of ^{119}Sn compounds of tetravalent tin with a tetrahedral system of Sn-IV chemical bonds (Bobokhuzhaev et al. 2020; Seregina et al. 1977). The ^{119}Sn spectra of the polycrystalline $\text{Ge}_2\text{Sb}_2\text{Te}_5$ samples in both phases, *fcc* and *hcp*, and of $\text{Ge}_{1.5}\text{Te}_{8.5}$ show isomer shifts $IS \sim 3.49\text{--}3.52$ mm/s, which are close to the isomer shift of the ^{119}Sn compound of divalent tin with tellurium, $IS = 3.55(2)$ mm/s, which has the octahedral system of chemical bonds.

The values of the isomer shift of the ^{119}Sn spectra suggest that tin atoms and germanium atoms replaced by tin atoms in the structural network of amorphous $\text{Ge}_2\text{Sb}_2\text{Te}_5$ and vitreous $\text{Ge}_{1.5}\text{Te}_{8.5}$ form a tetrahedral sp^3 system of chemical bonds. Because germanium (tin) atoms can have only tellurium atoms in their local environment in the structural network of the vitreous alloy, the close values of the isomer shift for all the amorphous materials under study indicate that germanium (tin) atoms are bonded only to tellurium atoms in the structural network of amorphous $\text{Ge}_2\text{Sb}_2\text{Te}_5$. The broadening of the ^{119}Sn spectra of all the amorphous materials under study is due to the lack of long-range order in the position of atoms in these materials—a characteristic property of the Mossbauer spectra of disordered structures.

The fact that the isomer shifts in the ^{119}Sn spectra of polycrystalline $\text{Ge}_2\text{Sb}_2\text{Te}_5$ and $\text{Ge}_{1.5}\text{Te}_{8.5}$ are close to those for the SnTe compound indicates that only tellurium atoms remain upon crystallization in the local environment of germanium (tin) atoms. The widths of the spectra of the polycrystalline samples substantially exceed the instrumental width. This indicates that tin does not form the SnTe compound (crystal lattice of NaCl type) in their composition, but enters into the composition of $\text{Ge}_{x-x}\text{Sn}_x\text{Te}$ solid solutions (in the $\text{Ge}_{1.5}\text{Te}_{8.5}$ alloy) or into the *fcc* or *hcp* phases (in $\text{Ge}_2\text{Sb}_2\text{Te}_5$ films). According to the X-ray diffraction data, the $\text{Ge}_{x-x}\text{Sn}_x\text{Te}$ solid solutions and the *fcc* $\text{Ge}_2\text{Sb}_2\text{Te}_5$ phase have rhombohedrally distorted lattices of the NaCl type, and the *hcp* $\text{Ge}_2\text{Sb}_2\text{Te}_5$ phase has a lattice with the 9-layered trigonal packing of atoms —Te—Sb—Te—Ge—Te—Te—Ge—Te—Sb— (Kato, Tanaka 2005; Shelby, Raoux 2009; Siegrist et al. 2011; Sousa 2011). Noncubic distortion of the lattices must lead to a quadrupole splitting of the Mossbauer spectra of ^{119}Sn by an amount that is smaller in the given case than the spectral line width.

Data of the emission Mossbauer spectroscopy on ^{119}Sn

In the process of the diffusion doping of $\text{Ge}_2\text{Sb}_2\text{Te}_5$ amorphous films with ^{119}Sb and ^{119m}Te impurity atoms at a temperature of ~ 300 °C, the films crystallize to give the *hcp* phase (Kato, Tanaka 2005; Shelby, Raoux 2009; Siegrist et al. 2011; Sousa 2011). The typical spectra of ^{119m}Sn impurity atoms formed

after the radioactive decay of ^{119}Sb atoms at antimony sites and ^{119m}Te at tellurium sites of the crystal lattice are presented in Fig. 4.

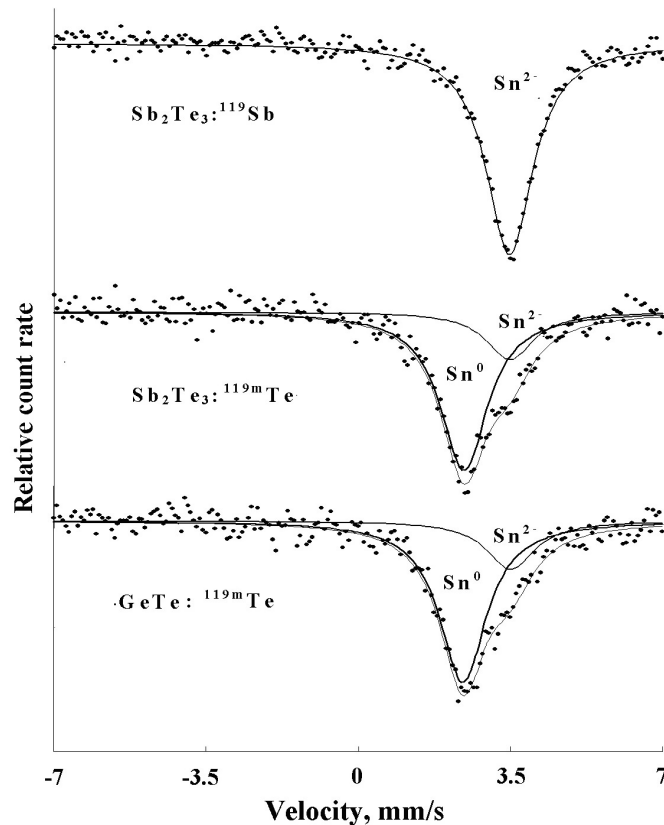


Fig. 4. Emission Mössbauer spectra of ^{119m}Sn impurity atoms formed after the radioactive decay of ^{119}Sb at antimony sites and ^{119m}Te at tellurium sites of a crystalline (*hcp*-phase) $\text{Ge}_2\text{Sb}_2\text{Te}_5$ film. The positions of spectral lines associated with Sn^{2+} and Sn^0 centers

In the case of ^{119}Sb parent atoms, the spectrum has the form of a single broadened line ($G = 1.32(2)$ mm/s). The isomer shift of this spectrum ($IS = 3.47(2)$ mm/s) corresponds to divalent tin Sn^{2+} . The spectrum of ^{119m}Sn impurity atoms formed upon the radioactive decay of ^{119}Sb parent atoms at antimony sites of the crystal lattice of Sb_2Te_3 has similar parameters. Hence follows the conclusion that, in both cases, tellurium atoms are in the local environment of $^{119m}\text{Sn}^{2+}$ atoms. This agrees with the data for the *hcp* structure of $\text{Ge}_2\text{Sb}_2\text{Te}_5$ crystalline films (Kato, Tanaka 2005), according to which tellurium atoms are in the local environment of antimony atoms. A conclusion can also be made that there are only tellurium atoms in the local environment of $^{119m}\text{Sn}^{2+}$ in both cases.

In the case of ^{119m}Te atoms, the spectrum is a superposition of two broadened lines ($G = 1.41\text{--}1.46$ mm/s). The higher intensity line with the isomer shift $IS = 2.42(2)$ mm/s falling within the range of isomer shifts of the spectra of intermetallic compounds of tin corresponds to $^{119m}\text{Sn}^0$ centers formed after the decay of ^{119m}Te mother atoms at tellurium sites. The layered lattice of the *hep* phase of $\text{Ge}_2\text{Sb}_2\text{Te}_5$ has three types of tellurium layers (Micoulaut et al. 2014), which gives rise to an inhomogeneous isomer shift in addition to a quadrupole splitting and significant broadening of the spectral line.

The weak intensity line with $IS = 3.51(2)$ mm/s is associated with $^{119m}\text{Sn}^{2+}$ centers formed after the decay of ^{119m}Te mother atoms shifted from tellurium sites to Sb or Ge sites due to the recoil energy accompanying the radioactive decay of the ^{119m}Te isotope. The set of sites to which the daughter atom of ^{119}Sb is shifted also leads to an inhomogeneous isomer shift and substantial broadening of the spectral line.

A similar structure is observed for the spectra of ^{119m}Sn impurity atoms formed after the radioactive decay of ^{119m}Te atoms at tellurium sites of the crystal lattices of Sb_2Te_3 and GeTe (see Fig. 5), and a conclusion can be made that only tellurium atoms are in all cases in the local environment of $^{119m}\text{Sn}^{2+}$ atoms.

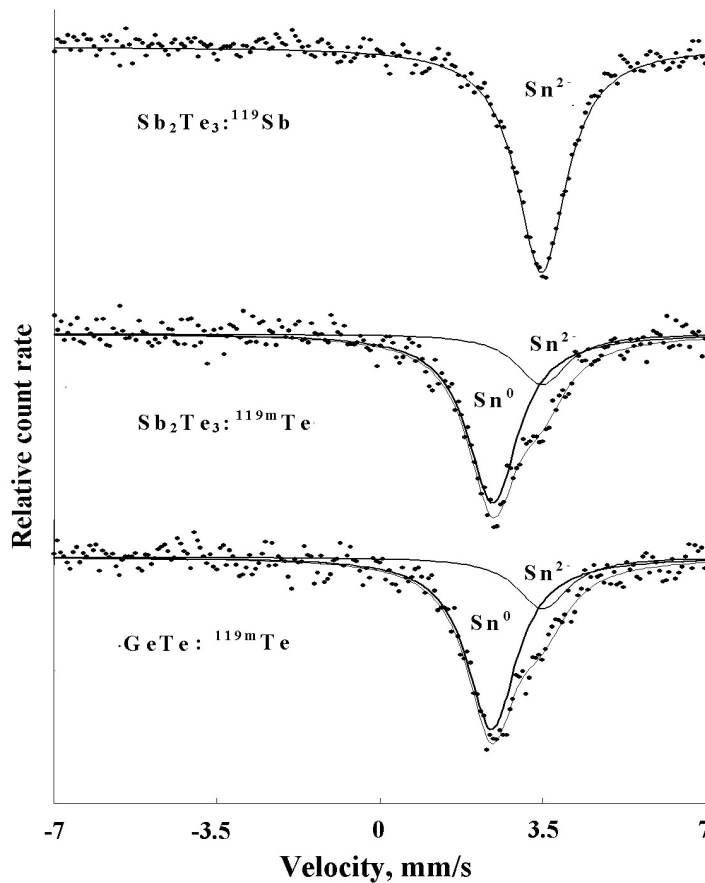


Fig. 5. Emission Mössbauer spectra of ^{119m}Sn impurity atoms formed after the radioactive decay of ^{119}Sb at antimony sites and ^{119m}Te at tellurium sites of the Sb_2Te_3 and GeTe compounds. The positions of spectral lines associated with Sn^{2+} and Sn^0 centers

The ^{119m}Sn atoms that are fixed, due to electron capture from ^{119}Sb or to a chain of electron-capture events from ^{119m}Te , at Sb or Te sites of the hep lattice of $\text{Ge}_2\text{Sb}_2\text{Te}_5$ can be regarded as models of antisite defects because an electronic analog of an atom from one sublattice (germanium) is found at the site of the other sublattice.

Conclusions

It was shown that tin atoms and germanium atoms substituting the former in the structure of amorphous and polycrystalline $\text{Ge}_2\text{Sb}_2\text{Te}_5$ and $\text{Ge}_{1.5}\text{Te}_{8.5}$ have different local environment symmetries (tetrahedral in the amorphous phase and octahedral in the crystalline phase). The method of emission Mössbauer spectroscopy on ^{119m}Sn impurity centers formed after the radioactive decay of ^{119}Sb and ^{119m}Te mother atoms was used to identify antisite tin defects at antimony and tellurium sites of $\text{Ge}_2\text{Sb}_2\text{Te}_5$ crystalline films. The broadening of the spectra of the antisite defects is accounted for either by a set of possible atoms (antimony, germanium, tellurium) in the local environment of tellurium sites, or by a similar set of sites to which the daughter ^{119}Sb atom is shifted.

References

- Bobokhuzhaev, K., Marchenko, A., Seregin, P. (2020) *Structural and antistructural defects in chalcogenide semiconductors. Mossbauer spectroscopy*. S. l.: LAP Lambert Academic Publ., 282 p. (In English)
- Hu, C., Yang, Z., Bi, C. et al. (2020) "All-crystalline" phase transition in nonmetal doped germanium–antimony–tellurium films for high-temperature non-volatile photonic applications. *Acta Materialia*, 188, 121–130. <https://doi.org/10.1016/j.actamat.2020.02.005> (In English)

- Kato, T., Tanaka, K. (2005) Electronic properties of amorphous and crystalline $\text{Ge}_2\text{Sb}_2\text{Te}_5$ films. *Japanese Journal of Applied Physics. Part 1: Regular Papers and Short Notes and Review Papers*, 44 (10R), 7340–7344. <https://doi.org/10.1143/JJAP.44.7340> (In English)
- Kolobov, A. V., Fons, P., Frenkel, A. I. et al. (2004) Understanding the phase-change mechanism of rewritable optical media. *Nature Materials*, 3 (10), 703–708. <https://doi.org/10.1038/nmat1215> (In English)
- Marchenko, A. V., Seregin, P. P., Terukov, E. I., Shakhovich, K. B. (2019) Antisite defects in Ge–Te and Ge–As–Te semiconductor glasses. *Semiconductors*, 53 (5), 711–716. <https://doi.org/10.1134/S1063782619050166> (In English)
- Micoulaut, M., Gunasekera, K., Ravindren, S., Boolchand, P. (2014) Quantitative measure of tetrahedral- sp^3 geometries in amorphous phase-change alloys. *Physical Review B*, 90 (9), article 094207. <https://doi.org/10.1103/PhysRevB.90.094207> (In English)
- Seregina, L. N., Nasredinov, F. S., Melekh, B. T. et al. (1977) Issledovanie lokal'noj struktury stekol v sistemakh kremnij-tellur, germanij-tellur i germanij-tellur-mysh'yak s pomoshch'yu messbauerovskoj spektroskopii na primesnykh atomakh olova [Study of the local structure of glasses in silicon-tellurium, germanium-tellurium and germanium-tellurium-arsenic systems using Mössbauer spectroscopy on impurity tin atoms]. *Fizika i khimiya stekla — Glass Physics and Chemistry*, 3 (4), 328–331. (In Russian)
- Shelby, R. M., Raoux, S. (2009) Crystallization dynamics of nitrogen-doped $\text{Ge}_2\text{Sb}_2\text{Te}_5$. *Journal of Applied Physics*, 105 (10), article 104902. <https://doi.org/10.1063/1.3126501> (In English)
- Siegrist, T., Jost, P., Volker, H. et al. (2011) Disorder-induced localization in crystalline phase-change materials. *Nature Materials*, 10 (3), 202–208. <https://doi.org/10.1038/nmat2934> (In English)
- Sousa, V. (2011) Chalcogenide materials and their application to Non-Volatile Memories. *Microelectronic Engineering*, 88 (5), 807–813. <https://doi.org/10.1016/j.mee.2010.06.042> (In English)